Tetrahedron: Asymmetry Vol. 4, No. 3, pp. 529-544, 1993
Printed in Great Britain

0957-4166/93 $6.00+.00
Pergamon Press Ltd

The Circular Dichroism of Oriented ß Sheets: Theoretical Predictions

Robert W. Woody

Department of Biochemistry
Colorado State University
Fort Collins, CO 80523

(*Received in UK* 21 *December* 1992)

This work is dedicated to the memory of Günther Snatzke.

Abstract: The CD tensor components for infinite planar antiparallel and parallel β sheets have been calculated. Exciton effects on the ππ transition and the nπ*-ππ* mixing are included. The results for all three principal directions are distinctly different, suggesting that CD should be useful for determining the orientation of β sheets in oriented proteins. The CD for light propagating normal to the plane of the sheet is very sensitive to the choice of center for the ππ* transition. For the antiparallel β sheet, the ππ* couplet reverses sign when this location is moved from the point on the NO line nearest the carbonyl carbon to the carbonyl carbon itself. For the parallel β sheet, the magnitude of the couplet increases by an order of magnitude for such a shift. The average CD is also affected by the choice of center, in that the sign of the long-wavelength ππ* exciton component is opposite for the two choices. While all previous calculations have used the point on the NO line, theoretical arguments support the choice of the carbonyl carbon. Further experimental data will be necessary to decide the issue. The present study sheds new light on the CD of idealized planar β sheets and provides predictions for the CD tensor properties of such sheets. The results should be useful for interpreting the CD of oriented membrane proteins with substantial quantities of β sheet.*

The circular dichroism of oriented α helices has been investigated both theoretically[1,2] and experimentally[3-6]. The characteristic differences between the CD measured along the helix axis and the average CD have proven useful in determining the orientation of helical segments in integral membrane proteins, such as bacteriorhodopsin[7], rhodopsin[8], cytochrome oxidase[9] and Ca^{+2}-dependent ATPase[10], and of a membrane-active antibiotic, alamethicin[11].

Since ß sheets are also important elements of secondary structure in proteins, it is important to characterize the CD tensor for such systems. The CD normal to the plane of the pleated sheet has been measured for films of poly(Leu-Lys)[12]. Relative to the average CD of the pleated sheet, the negative nπ* band at long wavelengths has a larger intensity, while the positive ππ* band near 195 nm is weaker.

The purpose of the present paper is to describe theoretical calculations of the components of the CD tensor for both the antiparallel and parallel ß sheets. A comparison of the results of these calculations with the one experimentally determined component of the CD tensor for the antiparallel ß sheet[12] demonstrates qualitative agreement. This suggests that the results presented here will be useful in the interpretation of the CD of oriented proteins containing significant amounts of ß sheet, such as porin[13]. The present paper also discusses some problems peculiar to theoretical calculations of the CD of ß sheets and suggests a possible reinterpretation of the average CD of the ß sheet.

THEORETICAL

Electrically allowed transitions

The rotational strength of the transition O → A for light propagating in the x-direction, $(R_{xx})_{OA}$, is given by[2,14]:

$$(R_{xx})_{OA} = (3e/2mc)\ \mathrm{Im}\ \{ (\mu_z)_{OA}\ (xp_y)_{AO} - (\mu_y)_{OA}(xp_z)_{AO} \} \quad (1)$$

Here $(\mu_y)_{OA}$ and $(\mu_z)_{OA}$ are components of the electric dipole transition moment, while $(xp_y)_{AO}$ and $(xp_z)_{AO}$ are components of the rp tensor, which is defined as:

$$(\mathbf{rp})_{AO} = \int \Psi_A^{*}\ \mathbf{rp}\ \Psi_o\ d\tau \quad (2)$$

where the dyadic $\mathbf{rp} = \Sigma \mathbf{r}_i\mathbf{p}_i$, and $\mathbf{r}_i$ and $\mathbf{p}_i$ are, respectively, the position and linear momentum of the *i*th electron. Corresponding expressions for the other diagonal elements of the rotational strength tensor, $(R_{yy})_{OA}$ and $(R_{zz})_{OA}$, can be obtained from Eqn (1) by cyclic permutation of x, y, and z.

In the case of an electrically allowed transition it is convenient to replace the momentum operator in Eqn. (2) by the electric dipole moment operator, leading to the equation[2,14]:

$$(R_{xx})_{OA} = 3\pi\upsilon_{OA}\ \{ (\mu_z)_{OA}(x\mu_y)_{OA} - (\mu_y)_{OA}(x\mu_z)_{OA} \} \quad (3)$$

where υ_{OA} is the frequency of the transition in cm^{-1}.

The electrically allowed $\pi\pi^*$ transition of the peptide group is treated by the exciton method[14-16], in which excited-state wavefunctions for the polypeptide are formulated as linear combinations of locally excited states:

$$\Psi_{OAK} = \sum_{i=1}^{n} C_{iAK}\Psi_{ia}\ ,\ K = 1,2,.....N. \quad (4)$$

Here Ψ_{OAK} is the wavefunction of the *K*th excited state, N is the number of identical peptide chromophores, and ψ_{ia} is the wavefunction for an excited state of the polymer in which residue *i* is excited to state *a*. The exciton coefficients for infinite ß sheets can be obtained by using cyclic boundary conditions[16]. Selection rules[17-19] give rise to only two and three allowed transitions in the parallel and antiparallel ß sheets, respectively. In infinite systems with helical symmetry, the selection rules for light propagating along the helix axis and for light incident normal to the helix axis are different [20-22]. This complication does not arise in the case of ß sheets, which have only two-fold symmetry elements. The exciton coefficients for the allowed transitions[17-18] in ß sheets are given in Table I.

Table I. Exciton Coefficients[a] for ß Sheets

Polarization	Antiparallel ß Sheets			
	c_1	c_2	c_3	c_4
x	1	-1	1	-1
y	1	1	-1	-1
z	1	-1	-1	1
-	1	1	1	1

Polarization	Parallel ß Sheets	
	c_1	c_2
xy	1	-1
y	1	1

a. The coefficients given here must be normalized before being used in Eqns. 4-8, $C_i = c_i/\sqrt{N}$.

The matrix elements for μ and for the $r\mu$ dyadic are expressed in terms of these exciton coefficients and the corresponding matrix elements for the monomer:

$$\mu_{OAK} = \sum_{i=1}^{N} C_{iAK}\, \mu_{ioa}, \tag{5}$$

$$(r\mu)_{OAK} = \sum_{i=1}^{N} C^{*}_{iAK}\, r_i \mu_{ioa} \tag{6}$$

where μ_{ioa} is the electric dipole transition moment for the transition $o \rightarrow a$ in group i, and r_i is the position vector for group i. Substitution of Eqns. (5) and (6) into Eqn. (3), combined with the recognition that the exciton coefficients are real, gives the equation:

$$(R_{xx})_{OAK} = 3\pi\nu_{oa}\sum_{i=1}^{N}\sum_{j>i}^{N} C_{iAK}\, C_{jAK}\, (x_j - x_i)\, \{(\mu_z)_{ioa}(\mu_y)_{joa} - (\mu_y)_{ioa}(\mu_z)_{joa}\} \tag{7}$$

This equation, given the exciton coefficients in Table I, and the ß sheet geometry, can be used to derive simple expressions for the rotational strength components of the parallel and antiparallel ß sheets. Schellman[19] derived such expressions in his treatment of vibrational excitons. The results are given in Table II for convenience, and because the coordinate system used here (Figure 1) differs from that used by Schellman.

Table II Rotational Strength Tensor Components for ß Sheets.

	Antiparallel ß Sheets - Exciton Components		
	x	y	z
(R_{xx})	0	$-3\pi\upsilon(x + a/4)\mu_y\mu_z$	$+3\pi\upsilon(x + a/4)\mu_y\mu_z$
(R_{yy})	$+3\pi\upsilon(y - b/4)\ \mu_x\mu_z$	0	$-3\pi\upsilon(y - b/4)\mu_x\mu_z$
(R_{zz})	$-3\pi\upsilon z\mu_x\mu_y$	$+3\pi\upsilon z\mu_x\mu_y$	0

	Parallel ß Sheets - Exciton Components	
	xz	y
(R_{xx})	$+3\pi\upsilon x\mu_z\mu_y$	$-3\pi\upsilon x\mu_z\mu_y$
(R_{yy})	0	0
(R_{zz})	$-3\pi\upsilon z\mu_x\mu_y$	$+3\pi\upsilon\ \mu_x\mu_y$

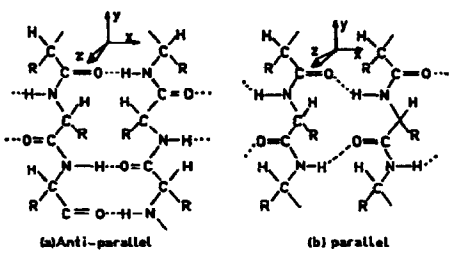

Figure 1. The coordinate system used for the calculations.

Electrically Forbidden Transitions

Exciton splitting of the $n\pi^*$ transition is negligible, but the $n\pi^*$ transition will mix to differing extents with the various $\pi\pi^*$ exciton components. Using first-order perturbation theory [10], the following expression can be derived for $(R_{xx})_{n\pi^*}$, considering only the mixing with a specific $\pi\pi^*$ exciton component:

$$(R_{xx})_{oa} = -\frac{e}{2mc}\sum_{i=1}^{N}\{\frac{2\nu_{OBK}}{h(\nu_{OBK}^2-\nu_{oa}^2)}\sum_{j\neq i}\sum_{k} C_{jbK}\, C_{kbK}\, V_{ioa\,;\,job}\ \mathrm{Im}\,[(\mu_z)_{iob}\,(xp_y)_{ioa} - \qquad (8)$$

$$(\mu_y)_{iob}(xp_z)_{ioa}] + \frac{1}{h(\nu_{OBK}-\nu_{oa})}\sum_{j\neq i}\sum_{k} C_{jbK}\, C_{kbK}\, V_{iob\,;\,joo}\ \mathrm{Im}\,[(\mu_z)_{iob}\,(xp_y)_{ioa} - (\mu_y)_{iob}(xp_z)_{ioa}]\}$$

This equation is analogous to Tinoco's[14] Eqn. (III B-31), except that Tinoco summed over all the exciton components of the electrically-allowed transition, so no exciton coefficients appear in his equation. In Eqn. (8), the transition o → a corresponds to the $n\pi^*$ transition, while o → b is the $\pi\pi^*$ transition, and K is a specific exciton component of the latter transition. $V_{ioa;job}$ is the Coulomb interaction between the $n\pi^*$ transition charge density in residue *i* and the $\pi\pi^*$ transition charge density in residue *j*, while $V_{iab;joo}$ is the interaction between the ground state charge density of group *j* and the transition charge density connecting the $n\pi^*$ and $\pi\pi^*$ excited states in residue *i*. Since both the o → a and a → b transitions are electrically forbidden, a monopole approximation[14] is used to calculate these Coulombic interactions. Cyclic permutations of the x,y, and z components in Eqn. (8) give expressions for the rotational strengths measured in the y and z directions. The mixing of $n\pi^*$ and $\pi\pi^*$ transitions also makes a contribution to the $\pi\pi^*$ rotational strength which is equal in magnitude but opposite in sign to that given in Eqn. (8), corresponding to an interchange of subscripts *a* and *b*.

The **rp** matrix elements in Eqn (8) must be evaluated theoretically, since the $n\pi^*$ transition is electrically forbidden. The matrix elements of (**rp**) are given in Table III for the antiparallel and parallel ß sheets.

Choice of Parameters

The geometry of ß poly (Ala), determined by Arnott *et al.* [24], was assumed for the antiparallel ß sheet. As noted by Snir *et al.*[25], the paper of Arnott *et al.*[24] does not correctly describe how to generate the adjacent antiparallel chain. The dyad axis which relates these two chains lies at (2.365, 0, 1.335) in the coordinate system used by Arnott *et al.* This differs slightly from the position inferred by Snir *et al.*[25] (2.365, 0, 1.27). The geometry used for the parallel ß sheet was that postulated by Pauling and Corey[26]. However, Pauling and Corey's coordinates refer to a polypeptide of D-amino acids. Therefore, the absolute configuration was inverted by reversing the sign of the z-coordinate.

Table III The **rp** Matrix[a] for the $n\pi^*$ Transition in Beta Sheets

Antiparallel ß sheet

$$\mathbf{rp} = \begin{pmatrix} 0 & 0.2096 & -0.0240 \\ -0.2096 & 0 & 0.9754 \\ 0.0240 & -0.9754 & 0 \end{pmatrix}$$

Parallel ß Sheet

$$\mathbf{rp} = \begin{pmatrix} 0 & -0.0243 & -0.1051 \\ 0.0243 & 0 & -0.9922 \\ 0.1051 & 0.9922 & 0 \end{pmatrix}$$

a. Units of Bohr magnetons. Coordinate system defined in Figure 1. Using amide wave functions of Woody[23].

The methods and parameters used for calculating the Coulomb interactions between the charge densities, transition and permanent, and the electric and magnetic dipole transition moments for the $\pi\pi^*$ and $n\pi^*$ transition were identical to those used previously[23,27]. The unperturbed $n\pi^*$ and $\pi\pi^*$ transition energies were taken to be 46080 cm^{-1} (217 nm) and 51020 cm^{-1} (196 nm) respectively. The $n\pi^*$ wavelength is that generally observed in the CD spectra of ß sheets[28]. The $\pi\pi^*$ wavelength was originally chosen[23] to give a good fit to the absorption and CD spectra of the α helix. The redshift from the usual wavelength for monomeric secondary amides (186 - 188 nm in water, 184-186 nm in cyclohexane)[29] and that of unordered polypeptides (192 nm)[30] can be attributed to environmental effects of the α helix. Denisov[31] has calculated these wavelength shifts and found a significant red shift for both the α helix and the ß sheets. Although Denisov's calculations give a somewhat smaller red shift for the ß sheets than for the α helix, the value of 196 nm used in previous calculations[27] has been retained.

The center chosen for the peptide $\pi\pi^*$ transition, which enters into Eqns (1) and (3), plays a pivotal role in these calculations. Two alternative choices have been used in this calculation--the point on the NO line lying closest to the carbonyl carbon[1] and the carbonyl carbon itself. The relative merits of these two choices will be discussed below. For convenience, they are referred to as the NO center and the C center, respectively.

RESULTS

Antiparallel ß sheets

The calculated rotational strengths for light propagating along each of the coordinate axes and the average rotational strengths for the antiparallel ß sheet are given in Table IV. Results are presented for

Table IV Calculated Rotational Strengths[a] for the Antiparallel ß Sheets

	$\pi\pi^*$ Exciton Components[b]			
	$n\pi^*$	x	y	z
λ(nm)[c]	217	196	201	184
(R_{xx})	-0.0020	0 0	0.0984 0.1442	-0.0964 -0.1422
(R_{yy})	-0.0494	0.8930 1.0347	0 0	-0.8436 -0.9853
(R_{zz})	-0.0542	0.3465 -0.2449	-0.2923 0.2991	0 0
(R)[d]	-0.0352	0.4132 0.2633	-0.0646 0.1478	-0.3133 -0.3758

a. The units are Debye-Bohr magnetons (DBM = 0.9273×10^{-38} cgs units).

b. The upper number is the rotational strength using the carbonyl carbon as the $\pi\pi^*$ center, while the lower is for the center on the NO-line.

c. The $n\pi^*$ wavelength is assumed to be 217 nm[28]. The $\pi\pi^*$ exciton components were calculated[27] assuming an unperturbed wavelength of 196 nm.

d. The average rotational strength, $(R) = [(R_{xx}) + (R_{yy}) + (R_{zz})]/3$.

both the centers considered for the $\pi\pi^*$ transition. Theoretical CD curves generated from the rotational strengths for light propagating in the z direction and for isotropic samples are shown in Figure 2. Gaussian band shapes with a uniform band width of 10 nm were assumed in generating these curves. Figure 2 also shows the average CD and the CD measured normal to the plane of the ß sheet for the alternating copolymer, poly(Leu-Lys)[12], compared with the corresponding theoretical curves.

The $n\pi^*$ rotational strengths do not depend on the choice of center for the $\pi\pi^*$ transition. The small (R_{xx}) predicted for the $n\pi^*$ transition is to be expected since the carbonyl bond direction, and hence $\mathbf{m}_{n\pi^*}$, is nearly parallel to the x-direction. Therefore, light propagating along the x-axis will only

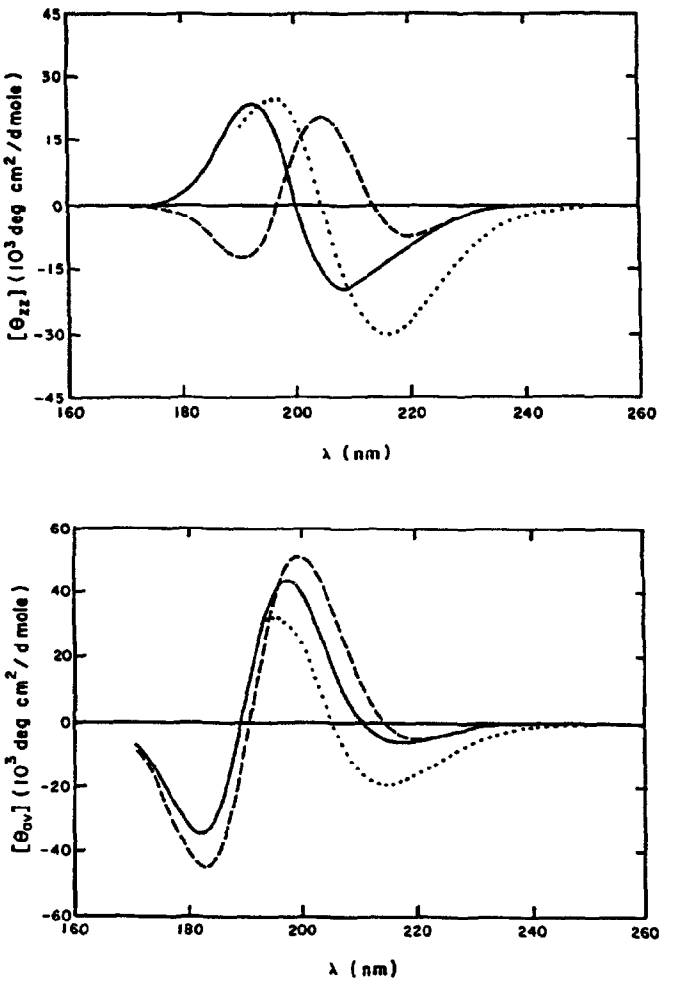

Figure 2. Theoretical and experimental CD curves for the antiparallel ß-sheet. Calculated CD spectra using C center (___) or N center (---). (a) [Θ_{zz}]; (b) [Θ_{av}]. Experimental CD spectra[12] (...) for poly (Leu-Lys) are also presented..

interact weakly with the $n\pi^*$ transition. (R_{yy}) and (R_{zz}) are much larger, negative, and comparable to each other. The average rotational strength calculated for the $n\pi^*$ transition in the infinite and antiparallel ß sheet (-0.0352 DBM) is consistent with the value previously calculated[27] for the largest finite sheet considered (-0.0403 DBM for a sheet 6 strands wide and 8 residues long).

For the $\pi\pi^*$ transition, (R_{xx}) is also small, consistent with the fact that the $\pi\pi^*$ transition has its largest component along the x-direction. (R_{yy}) has the largest rotational strengths for the $\pi\pi^*$ transition. In this case, the large x component of the $\pi\pi$ transition can combine with the large difference in y coordinates between centers in the unit cell (Eqn. (3)). (R_{zz}) is relatively small, despite the fact that it involves the two largest components of the $\pi\pi^*$ transition, μ_x and μ_y. This is attributable to the small extent of the pleated sheet in the z direction, which gives (coincidentally) a center-to-center distance of 0.26 Å for either choice of center for the $\pi\pi^*$ transition. For all three directions, the calculated $\pi\pi^*$ rotational strengths for the two non-zero exciton components are opposite in sign and nearly equal in magnitude. The small differences in magnitude are due to unequal contributions from mixing with the $n\pi^*$ transition. Thus a CD couplet[32] is predicted in the $\pi\pi^*$ region for the CD measured along each of the coordinate axes. The couplet is expected to be positive for the x and y directions, while for the z component the sign of the couplet depends on the choice of the $\pi\pi^*$ center.

The choice of center for the $\pi\pi^*$ transition does not strongly affect the value of R_{yy} (*ca.* 15% difference between the two positions considered here). R_{xx} is more strongly affected, with a *ca.* 50% difference. However R_{zz} is reversed in sign when the origin is shifted from the carbonyl carbon to the NO line. Earlier calculations of the average CD of the ß sheet[17,27,33-35] used the center located on the NO line at the point nearest the carbonyl carbon, which was initially chosen arbitrarily[1]. The carbonyl carbon itself provides an equally plausible choice for the center of the peptide group. In the ß sheet, these two centers lie on opposite sides of the xy plane and thus have z coordinates of opposite sign. Therefore, the predicted sign of the exciton components for R_{zz} is opposite for these two choices of the peptide center. This difficulty was not appreciated in the earlier calculations on ß sheets, but was noted by Schellman and coworkers[25] in their calculations of the vibrational CD of ß sheets. As noted by Snir *et al.*[25], the problem arises because the axis of the two-fold helix, which corresponds to the chain direction in the ß sheet, passes through the peptide group. By contrast, the predicted CD of the α helix is insensitive to the choice of the peptide center because the plane of the peptide is well-removed (*ca.* 1.5 Å) from the helix axis and is nearly parallel to the axis.

Parallel ß sheets

The calculated rotational strength tensor components and the average rotational strength for infinite parallel ß sheets are presented in Table V. Theoretical CD spectra generated from these rotational strengths and theoretical transition energies[27] are shown in Figure 3.

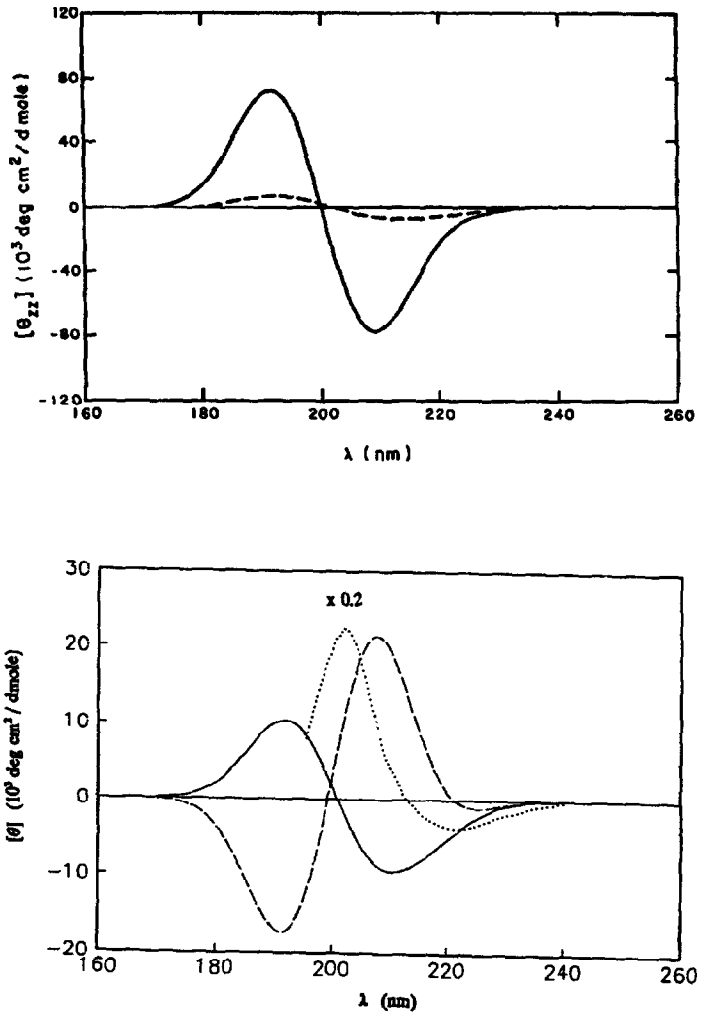

Figure 3. Theoretical and experimental CD curves for the parallel ß-Sheet. Calculated CD spectra using C center (___) or N center (---). (a) $[\Theta_{zz}]$; (b) $[\Theta_{av}]$. Experimental data[36] (...) for $(L\text{-Ile})_7$ are shown for the average CD. Note that the experimental spectrum has been reduced by a factor of 0.2.

Table V Calculated Rotational Strengths[a] for the Parallel ß Sheet

	$\pi\pi^*$ Exciton Components		
	$n\pi^*$	xz	y
λ(nm)[c]	217	193	207
(R_{xx})	0.0018	-0.3678 -0.5100	0.3660 0.5082
(R_{yy})	-0.0383	0.0383 0.0383	0 0
(R_{zz})	-0.0371	0.5652 0.0537	-0.5280 -0.0165
(R)[d]	-0.0245	0.0786 -0.1393	-0.0540 0.1639

a - d. See footnotes to Table IV.

The $n\pi^*$ rotational strengths are comparable to those for the antiparallel β sheet for each component, so the comments made for the antiparallel case hold here also. The average rotational strength for the infinite parallel ß sheet (-0.0245 DBM) agrees reasonably well with that for the largest finite sheet considered previously (-0.0167 DBM).

The $\pi\pi^*$ exciton components for the parallel ß sheets are significantly different from those for the antiparallel form. This is largely due to the fact that there are only two allowed components for the parallel sheet. $\pi\pi^*$ couplets are predicted for (R_{xx}) and (R_{zz}). The (R_{xx}) couplet is decreased in magnitude by *ca.* 30% on changing from the NO center to the C center, but the (R_{zz}) couplet increases by roughly an order of magnitude. The most striking difference with respect to the antiparallel ß sheet is in (R_{yy}), which is extremely weak, with no $\pi\pi^*$ exciton contribution and only a small positive rotational strength in the xz component resulting from mixing with the $n\pi^*$ transition. In the antiparallel ß sheet, (R_{yy}) is the strongest of the components. The difference is a result of the fusion of the x and z components of the antiparallel ß sheet into a single xz component in the parallel ß sheet. If measurement along the chain direction were feasible, the parallel and antiparallel ß sheets would be readily distinguishable.

The average CD of the parallel ß sheet also depends on the choice of $\pi\pi^*$ center. For the C center, as shown in Figure 3b, the negative $n\pi^*$ band merges with the negative y polarized exciton component to give a negative couplet with extrema near 210 and 190 nm. The average CD obtained with an NO center, by contrast, has a very weak negative $n\pi^*$ band, followed by a positive $\pi\pi^*$, also with extrema near 210 and 190 nm. These theoretical results are compared in Figure 3b with experimental

data[36] for $(L\text{-Ile})_7$. Toniolo, Stevens and coworkers have provided infrared[37] and CD[38] evidence that the heptamers (and, in some cases, lower oligomers) of these amino acids form sheets in the solid state or in solution at high concentrations which are predominantly parallel ß sheets.

DISCUSSION

Acute sensitivity of the calculated CD to the choice of location for the center of a transition is unusual, but not unprecedented. An especially instructive example is that of 1,5-disubstituted-9, 10-dihydro-9, 10- ethenoanthracenes. Tanaka and coworkers[39] reported that exciton calculations on such systems, based upon the absolute configuration determined by X-ray diffraction, predicted CD spectra opposite in sign to those observed. Tanaka *et al.*[39] questioned the validity of the widely accepted Bijvoet[40] method for determining absolute configurations by X-ray diffraction. However, Mason[41] and Hezemans and Groenewege[42] showed that the apparent discrepancy between exciton theory and the experimental CD resulted from the choice of origin for the monomer transitions. Tanaka and coworkers had taken the origin to be shifted from the center of the benzene rings *toward* the substituents, as is predicted by the dipole length formalism, i.e. using the r operator for electric dipole transition moments. As first recognized by Moffitt[16], the dipole velocity method, using ∇ or p matrix elements, avoids the origin-dependence of rotational strengths inherent in the dipole length method. In the dipole velocity approximation, the center for a monosubstituted benzene ring is shifted *away* from the substituent rather than toward it. If one uses the dipole velocity method to ascertain the location of the $\pi\pi^*$ transitions in the ethenoanthracenes, the exciton theory gives results consistent with experiment for the absolute configuration derived from X-ray diffraction.

In discussing this problem, Mason[41] gave a useful heuristic approach to determining the location of the appropriate center for $\pi\pi^*$ transitions. This method is applied to the present problem in Figure 4. For simplicity, the isoelectronic carboxylate group is used because of its higher symmetry. The crucial point is that dipole length matrix elements are dominated by one-center contributions, while in dipole velocity matrix elements, the one-center contributions vanish, and two-center contributions between nearest neighbors dominate. The center-of gravity for the transition monopoles, which determine the dipole length matrix element, lies halfway between the oxygens in the carboxylate group, and will be close to the midpoint of the N-O line in amides. The arbitrary NO center previously used for the peptide group corresponds closely to the dipole length center. By contrast, the dipole velocity vectors have their center-of-gravity at the carbonyl carbon in the carboxylate group and presumably near this point in amides.

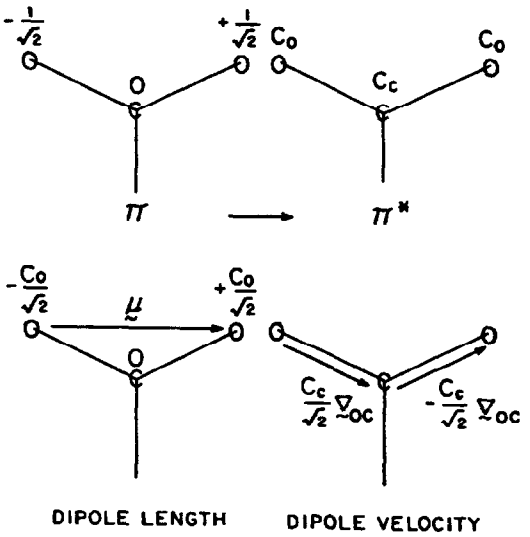

Figure 4. Choice of origin of the $\pi\pi^*$ transition using the carboxylate group as a model for amides. (a) Dipole length method; (b) dipole velocity method.

Another approach to this problem was proposed by Stiles[43]. The origin for a transition can be chosen arbitrarily, so long as one takes the angular momentum or magnetic moment of the transition about that origin into account. However, the equations are considerably simpler if electrically allowed transitions, such as $\pi\pi^*$ transitions, are assigned origins such that their magnetic moment vanishes. π-electron and CNDO/S MO calculations on the amide group (data not shown) give a vanishing or very small magnetic dipole transition moment for the first $\pi\pi^*$ transition when the origin is chosen at the carbonyl carbon, but a significant out-of-plane magnetic moment when the origin is at the NO center.

These theoretical arguments support the choice of the carbonyl carbon as the center for the $\pi\pi^*$ transition. A comparison of the theoretical and experimental CD of the antiparallel β sheet measured along the z-direction (Figure 2a) appears to provide further support. While neither theoretical curve gives a perfect fit to the experimental data, the agreement using the C center is better. For example, it yields roughly comparable magnitudes for the long-wavelength negative band and the short-wavelength positive band, in agreement with experiment, while the calculation using the NO center predicts about a three-fold difference in magnitude. The positions of the extrema and the crossover near 200 nm are also reproduced better by the C-center calculation. Finally, the NO-center calculation predicts a

crossover to negative CD at 196nm whereas, experimentally, the CD is near its positive maximum and remains positive to the lower limit of the measurements, near 185 nm. The average CD spectra for the antiparallel sheet, calculated and observed, are illustrated in Figure 2b. In this case, the choice between the two calculated curves is not clear cut. The C-center calculation is marginally better in reproducing the amplitude of both observed extrema and the crossover wavelength observed at 205 nm.

It must be recalled in this and subsequent comparisons with experimental data that the present theoretical results refer to an infinite planar structure. Edge effects and nonplanarity[44-46] (twisting) of the pleated sheet will lead to quantitative and perhaps qualitative changes in the predicted spectra. Furthermore, the calculations neglect the contributions of higher energy transitions. Moreover, the choice of 196 nm as the wavelength at which the $\pi\pi^*$ excitation band for the antiparallel sheet is centered is somewhat arbitrary. If the center-of-gravity were shifted by 4-6 nm to the blue, the agreement of the NO-center calculations with experiment would be significantly improved, while that for the C-center calculations would be less satisfactory. Uncertainty in the appropriate unperturbed energy for the $\pi\pi^*$ transition, combined with the limits in the present calculations imposed by neglect of twisting in the ß sheet and/or higher energy transitions, make a definitive comparison with experiment premature. Calculations of the average CD for twisted ß sheets have been performed[47] (Illangasekare and Woody, in preparation). The predicted CD spectra of slightly twisted antiparallel sheets, such as those predicted for poly (L-Ala) by Chou and Scheraga [48] are in good agreement with those predicted here for planar sheets, and also agree well with the spectra observed for poly (L-Lys)[28] and poly (Leu-Lys)[12]. Thus, the present calculations should give a good approximation for the directional properties of such systems. By contrast, the average CD of strongly twisted antiparallel ß sheets are predicted to show a much stronger positive band near 200nm and a strong negative band near 180 nm.

Based on the earlier calculations[17,27,33-35], the generally accepted interpretation[49] of the CD of ß sheets is that the negative long-wavelength band is due only to the $n\pi^*$ transition, while the positive band in the 195-200 nm region contains positive contributions from both the x- and y-polarized exciton bands. If the NO center used in the previous studies is replaced by the C center, this view is altered. The y-polarized exciton band is weak but negative, and contributes to the long-wavelength negative band, rather than the positive 195-200 nm band, which is solely due to the x-polarized exciton band.

The only direct experimental evidence supporting the presence of two positive bands in the $\pi\pi^*$ region is the observation[50] of two positive components in the CD spectrum of poly(L-Lys) in the presence of 0.12 M sodium dodecyl sulfate (SDS). Such a resolution into two components has not been reported in any other form of the ß sheet. The conformation and/or the optical properties of poly(L-Lys) in the ß form may be substantially perturbed by the presence of the detergent. For example, the amplitude of the 217 nm band for the detergent-induced form is reduced by about a factor of two relative to that of poly(L-Lys) in aqueous solutions. Li and Spector[51] have proposed that the differences in properties of

the SDS-induced ß form of the poly(L-Lys) and that induced by heating at high pH result from differences in the size of the ß sheet, with the latter giving rise to much larger sheets. The band positions observed by Timasheff *et al.*[50] for the detergent-induced ß form (190 and 197 nm) would be consistent with those predicted[27] for a two-stranded ß structure.

If an integral membrane protein has a large antiparallel ß sheet content, and if the sheet has a predominant orientation with respect to the plane of the membrane, CD measurements should permit the determination of this orientation. A negative $\pi\pi^*$ couplet implies that the sheet is oriented parallel to the plane of the membrane and that the C-center model is correct. A strong, positive $\pi\pi^*$ couplet (couplet strength ~ + 2 x 10^5 deg cm^2/dmole) indicates that the plane of the sheet is normal to the membrane, with the chain direction aligned with the normal. A weak positive $\pi\pi^*$ couplet (couplet strength ~ + 25 x 10^3 deg cm^2/dmole) implies that the plane is normal to the membrane, but with the chain direction parallel to the plane of the membrane or that the plane is parallel to the membrane and the NO-center model is correct. These inferences can be tested by infrared linear dichroism. A combination of the two measurements might provide information on ß sheets with arbitrary orientations.

The shape of the CD spectrum calculated for the parallel β sheet with the NO center (Figure 3b) agrees better with the experimental data[36] than that for the C center, although the amplitude differs by at least a factor of five, and the experimental spectrum is blue-shifted by *ca.* 5 nm. However, the experimental data refer to what is almost certainly a strongly twisted ß sheet. The conformational energy calculations of Chou *et al.*[52] show that the ß branched amino acids form parallel ß sheets in preference to antiparallel sheets and that these sheets are, in contrast to the antiparallel sheet of poly (L-Ala), very strongly twisted. Thus, the only experimental models we currently have for parallel ß sheets deviate strongly from the planar structure treated in this paper, and therefore we cannot use the data on $(L\text{-Ile})_7$ or $(L\text{-Val})_7$ to decide between the two centers.

Thus, at present, an unambiguous distinction between the two choices of center for the $\pi\pi^*$ transition based upon comparison of theory and experiment is not possible. The theoretical arguments described above support the C-center, but the conclusion from the experimental data is at present unclear. Further experimental data on oriented systems will be helpful. For example, extension of the measurements[12] on oriented films of poly (Lys-Leu) to shorter wavelengths could provide stronger support for one model or the other, depending on whether a negative band is seen near 180 nm (see Figure 2a). Calculations need to be extended by incorporation of the effects of higher energy transitions, application to other oligo- and polypeptide systems such as ß turns and cyclic peptides, and analysis of average and oriented CD of twisted ß sheets.

In summary, the present results provide the first analysis of the oriented CD of ß sheets in the far ultraviolet. Although the model assumes a planar structure, many of the model ß sheets with amino acids lacking branching at the ß carbon appear to form antiparallel structures which deviate only slightly from

this idealized structure. The few parallel ß sheet models deviate from it strongly, however. The results demonstrate a sensitivity to the choice of transition center and suggest that some reinterpretation of ß sheet CD may be necessary.

ACKNOWLEDGEMENTS

The author is grateful to Drs. Mali Illangasekare and Mohammed Bazzi for helpful discussions. This work was supported by USPHS Grant GM22994.

REFERENCES

1. Woody, R. W.; Tinoco, I., Jr. *J. Chem. Phys.* **1967**, *46*, 4927-4945.
2. Snir, J.; Schellman, J. *J. Phys. Chem.* **1973**, *77*, 1653-1661.
3. Hoffman, S. J.; Ullman, R. *J. Polymer Sci., Part C* **1970**, *31*, 205-215.
4. Mandel, R.; Holzwarth, G. *J. Chem. Phys.* **1972**, *57*, 3469-3477.
5. Olah, G. A.; Huang, H. W. *J. Chem. Phys.* **1988**, *89*, 2531-2537.
6. Olah, G. A.; Huang, H. W. *J. Chem. Phys.* **1988**, *89*, 6956-6962.
7. Muccio, D. D.; Cassim, J. Y. *Biophys. J.* **1979**, *26*, 427-440.
8. Rothschild, K. J.; Sanches, R.; Hsiao, T. L.; Clark, N. A. *Biophys. J.* **1980**, *31*, 53-64.
9. Bazzi, M. D.; Woody, R. W. *Biophys J.* **1985**, *48*, 957-966.
10. Bazzi, M. D. *Orientation of Cytochrome Oxidase, Ca^{+2}-ATPase, and Poly (Leu-Lys) in Membranes: A CD and IR Study*, Colorado State University 1984.
11. Wu, Y.; Huang, H. W.; Olah, G. A. *Biophys. J.* **1990**, *57*, 797-806.
12. Bazzi, M. D.; Woody, R. W.; Brack, A. *Biopolymers*, **1987**, *26*, 1115-1124.
13. Weiss, M. S.; Schulz, G. E. *J. Mol. Biol.* **1992**, *227*, 493-509.
14. Tinoco, I., Jr. *Adv. Chem. Phys.* **1962**, *4*, 113-160.
15. Davydov, A. S. *Theory of Molecular Excitons*, Dresner, S.B., Transl., Plenum Press, New York, 1971.
16. Moffitt, W. *J. Chem. Phys.* **1956**, *25*, 467-478.
17. Pysh, E. S. (1966) *Proc. Natl. Acad. Sci. USA*. **1966**, *56*, 825-832.
18. Rosenheck, K.; Sommer, B. (1967) *J. Chem. Phys.* **1967**, *46*, 532-536.
19. Schellman, J. A. In *Peptides, Polypeptides, and Proteins*, Blout, E.R.; Bovey, F.A.; Goodman, M.; Lotan, N., eds., John Wiley and Sons, New York, 1974, pp. 320-337.
20. Ando, T. *Prog. Theor. Phys. (Kyoto)* **1968**, *40*, 471-485.
21. Loxsom, F. M. *J. Chem. Phys.* **1969**, *51*, 4899-4905.

22. Deutsche, C. W. *J. Chem. Phys.* **1970**, *52*, 3703-3714.
23. Woody, R. W. *J. Chem. Phys.* **1968**, *49*, 4797-4806.
24. Arnott, S.; Dover, S. D.; Elliott, A. *J. Mol. Biol.* **1967**, *30*, 201-208.
25. Snir, J.; Frankel, R. A.; Schellman, J.A. *Biopolymers* **1975**, *14*, 173-196.
26. Pauling, L.; Corey, R. B. *Proc. Natl. Acad. Sci. USA* **1953**, *39*, 253-256.
27. Woody, R. W. *Biopolymers* **1969**, *8*, 669-683.
28. Greenfield, N.; Fasman, G.D. *Biochemistry* **1969**, *8*, 4108-4116.
29. Nielsen, E. B.; Schellman, J. A. *J. Phys. Chem.* **1967**, *71*, 2297-2304.
30. Rosenheck, K.; Doty, P. *Proc. Natl. Acad. Sci. USA.* **1961**, *47*, 1775-1785.
31. Denisov, D. A. *Biophysics* (Engl. transl. of *Biofizika*) **1969**, *14*, 11-16.
32. Schellman, J. A. *Accts. Chem. Res.* **1968**, *1*, 144-151.
33. Zubkov, V. A.; Vol'kenshtein, M. V. *Mol. Biol.* (Engl. transl. of *Molek. Biol.*) **1970**, *4*, 483-489.
34. Pysh, E. S. *J. Chem. Phys.* **1970**, *52*, 4723-4733.
35. Madison, V.; Schellman, J. *Biopolymers* **1972**, *11*, 1041-1076.
36. Toniolo, C.; Bonora, G. M.; Fontana, A. *Intl. J. Pept. Protein Res.* **1974**, *6*, 371-380.
37. Toniolo, C.; Palumbo, M. *Biopolymers* **1977**, *16*, 219-224.
38. Balcerski, J. S.; Pysh, E. S.; Bonora, G. M.; Toniolo, C. *J. Am. Chem. Soc.* **1976**, *98*, 3470-3473.
39. Tanaka, J.; Katayama, C.; Ogura, F.; Tatemitsu, H.; and Nakaga, M. *J. Chem. Soc. Chem. Comm.* **1973**, 21-22.
40. Bijvoet, J. M.; Peerdeman, A. F.; van Bommel, A. J. *Nature* **1951**, *168*, 271-272.
41. Mason, S. F. *J. Chem. Soc. Chem. Comm.* **1973**, 239-241.
42. Hezemans, A. M. F.; Groenewege, M. P. *Tetrahedron* **1973**, *29*, 1223-1226.
43. Stiles, P. J. *Mol. Phys.* **1971**, *22*, 731-732.
44. Chothia, C. *J. Mol. Biol.* **1973**, *75*, 295-302.
45. Richardson, J. S. *Adv. Protein Chem.* **1981**, *34*, 167-339.
46. Salemme, F. R. *Prog. Biophys. Mol. Biol.* **1983**, *42*, 95-133.
47. Manning, M. C.; Illangasekare, M.; Woody, R. W. *Biophys. Chem.* **1988**, *31*, 77-86.
48. Chou, K. C.; Scheraga, H. A. *J. Mol. Biol.* **1982**, *162*, 89-112.
49. Woody, R. W. *J. Polym. Sci. Macromol. Rev.* **1979**, *12*, 181-321.
50. Timasheff, S. N.; Susi, H.; Townend, R.; Stevens, L.; Gorbunoff, M. N.; Kumosinski, T. F. In *Conformation of Biopolymers*, Ramachandran, G. N. ed.; Academic Press, London, 1967, Vol. 1, pp. 173-196.
51. Li, L. K.; Spector, A. *J. Am. Chem. Soc.* **1969**, *91*, 220-222.
52. Chou, K. C.; Nemethy, G.; Scheraga, H. A. *J. Mol. Biol.* **1983**, *168*, 389-407.